Computational and Experimental Insights into the Antiviral Mechanism of Turmeric (*Curcuma longa*) against SARS-CoV-2 D614G

Hagar Ali Marzouk[1], *Marlita* Marlita[2,3], *Kavana Hafil* Kusuma[1], *Yuyun Ika* Christina[4,5], *Aries* Soewondo[6], *Sri* Rahayu[6], *Nashi* Widodo[4,5,6], and *Muhammad Sasmito* Djati[4,5,6,*]

[1]Doctoral Program, Department of Biology, Faculty of Mathematics and Natural Sciences, Brawijaya University, Malang 65145, East Java, Indonesia
[2]Faculty of Mechatronics, Informatics and Interdisciplinary Studies, Technical University of Liberec, Studentská 1402/2, 461 17 Liberec, Czech Republic
[3]Institute for Nanomaterials, Advanced Technologies and Innovation, Technical University of Liberec, Bendlova 1409/7, 461 17 Liberec, Czech Republic
[4]Innovation Center of Integrative Jamu and Eco-pharmaca, Brawijaya University, Malang 65145, East Java, Indonesia
[5]Dewan Jamu Indonesia East Java Region, Malang, East Java, Indonesia
[6]Department of Biology, Faculty of Mathematics and Natural Sciences, Brawijaya University, Malang 65145, East Java, Indonesia

Abstract. Natural plant-derived compounds are increasingly investigated as potential inhibitors of SARS-CoV-2 infection. Turmeric (*Curcuma longa*) contains curcumin and other bioactive compounds with reported antiviral, anti-inflammatory, and immunomodulatory properties. However, the inhibitory mechanism of *C. longa* against SARS-CoV-2 D614G virus-like particles (VLPs) has not been fully elucidated. This study aimed to evaluate the potential of the ethanol extract of *C. longa* to inhibit viral entry through integrated *in silico* and *in vitro* approaches. Liquid Chromatography-High Resolution Mass Spectrometry (LC-HRMS) analysis identified 24 major bioactive compounds, which were screened for drug-likeness and predicted antiviral activity using PASS Online. Molecular docking was performed using PyRx software by targeting the receptor-binding domain (RBD) of the SARS-CoV-2 spike glycoprotein, followed by 20-ns molecular dynamics simulations to evaluate complex stability. For in vitro validation, Vero E6 cells were exposed to SARS-CoV-2 D614G VLPs expressing EGFP reporter and turmeric extract (2.5 and 5 µg/mL). Viral entry was quantified by EGFP fluorescence intensity after 24 h. The results showed that cyclobisdemethoxycurcumin and curcumin showed high binding affinity (−7.035 and −6.258 kcal/mol, respectively) and stable interactions within the RBD binding pocket. Treatment with *C. longa* extract significantly ($p < 0.05$) inhibited VLP internalization into Vero E6 compared with the untreated control. These findings demonstrate that *C. longa* bioactive compounds interfere with SARS-CoV-2 D614G spike-mediated

* Corresponding author: msdjati@ub.ac.id

entry. Therefore, it can support their potential as natural antiviral candidates for further in vitro and in vivo investigation.

1 Introduction

The severity and death rate of the COVID-19 disease have significantly declined since global vaccination programs and antiviral treatments have significantly lowered the death rates. Nevertheless, SARS-CoV-2 continues to spread across the globe and develop new strains almost every week, which indicates that it remains relevant to the health of people [1]. Hence, the reason why more research is required is not because the pandemic remains in its most severe stage, but rather because the virus may continue to evolve and trigger new outbreaks, particularly in the form of mutations that will alter the ease with which the virus may spread, as well as the effectiveness with which the immune system can react to the virus [2]. Particularly, modifications in the spike (S) protein are very significant to render viruses more contagious and easier to be neglected by the immune system. This continues to complicate the effectiveness of vaccines against viruses in the long run, and to develop new strategies against viruses. In addition, the discovery of antiviral medications against SARS-CoV-2 might be applicable in the treatment of other severe respiratory diseases, such as ISPA or seasonal flu [3]. Such re-framing appeals to the modern post-pandemic reality and the practical and scientific need to conduct further research.

Virus-like particles (VLPs) have gained attention in this context as potential candidates for vaccine development, offering a safe and effective approach to elicit immune responses without the risk associated with live viruses [4]. These VLPs mimic the structure of the virus and are engineered to express viral antigens, which can provoke a protective immune response against natural infections, thereby providing immunity in a controlled manner. Notably, the D614G mutation in the SARS-CoV-2 spike protein has been associated with increased viral entry efficiency and transmissibility. This mutation exemplifies the dynamic nature of SARS-CoV-2, as it evolves in response to host immune pressures, leading to variants that may partially escape neutralizing antibodies. Such mutations call for continuous monitoring and adaptation of therapeutic and preventative measures, making it essential to explore innovative strategies to counteract viral evolution and bolster vaccine efficacy. Research has indicated that vaccine platforms utilizing SARS-CoV-2 VLPs can be effective against these mutations, showcasing their versatility in addressing emergent variants [5].

In this context, natural products have attracted considerable interest as potential sources of antiviral agents. Turmeric (*Curcuma longa*), a medicinal plant widely used in traditional medicine, contains curcumin and related polyphenolic compounds known for their broad-spectrum biological activities, including antiviral, anti-inflammatory, and antioxidant effects. Several studies have suggested that curcumin may interfere with viral replication and mitigate the excessive inflammatory response associated with severe COVID-19, often referred to as the cytokine storm. The integration of VLP-based assays with turmeric-derived compounds provides a promising framework to evaluate both viral entry inhibition and immune-modulatory potential.

Despite the widespread use of *C. longa*, scientific evidence regarding its effectiveness in preventing and treating SARS-CoV-2 is still limited, with most findings based only on in vitro antiviral activity [6] and in silico predictions of viral protein inhibition rather than confirmed clinical outcomes [7]. Therefore, this study aimed to investigate the effect of turmeric (*C. longa*) extract on the entry of SARS-CoV-2 D614G virus-like particles (VLPs) using an integrated in silico and in vitro approach. Molecular docking and dynamics simulations were employed to assess the binding affinity of turmeric-derived compounds toward the spike protein receptor-binding domain (RBD), followed by validation through VLP-based entry inhibition assays in Vero E6 cells, a kidney epithelial cell line from African green monkey commonly used for SARS-CoV-2 entry studies due to its high ACE2 expression.

2 Material and Method

2.1 Extraction of *C. longa* and Liquid chromatography high-resolution mass spectrophotometry (LC-HRMS) analysis

The powdered turmeric (*C. longa*) was purchased from UPT. Balai Materia Medica in Batu, East Java. The extraction procedure used the maceration technique with ethanol. For a 48-hour maceration, 900 mL of 96% methanol was combined with *C. longa* powder. The solvent was evaporated and then replenished twice at room temperature. Whatman filter paper No. 41 was used to filter the resultant macerate. The filtrate was then evaporated at a temperature between 50 and 60°C using a rotary evaporator (Buchi R-114). After that, the finished extract was kept at 4°C in a refrigerator.

2.2 Liquid chromatography high-resolution mass spectrophotometry (LC-HRMS) analysis

LC–HRMS analysis was performed following an adapted protocol from previous study. A 10 mg portion of each sample was injected into a Thermo Scientific Vanquish UHPLC system coupled to an Orbitrap HRMS. Separation was achieved using an Accucore Phenyl-Hexyl column (100 × 2.1 mm, 2.6 μm) with a water (0.1% formic acid)–methanol (0.1% formic acid) gradient at 0.3 mL/min. The gradient started at 5% B, increased to 90% within 16 min, held for 4 min, and re-equilibrated to initial conditions. The system operated at 40°C with a 3 μL injection volume. Untargeted data were acquired in full MS and dd-MS² modes under positive and negative ionization. Nitrogen served as all gas supplies, with a spray voltage of 3.30 kV and temperatures of 320°C (capillary) and 30°C (auxiliary). Mass spectra were collected over 66.7–1000 m/z using resolutions of 70,000 (full MS) and 17,500 (dd-MS²). Mass accuracy was evaluated using the Warwick Mass Error calculator.

2.3 In silico study

2.3.1 Drug likeness and Antiviral Activity Screening

SwissADME (https://www.swissadme.ch/) was used to screen bioactive compounds for drug-likeness and potential activity, utilizing standards like Veber, Egan, and Lipinski's rule of five. These compounds may be more attractive therapeutic candidates if they have a higher drug-likeness score. The PASS Prediction of Activity Spectra for Substances service (http://way2drug.com/passonline/) was used to assess the bioactivity of compounds that satisfied the screening requirements. SMILES from the PubChem database were used in the predictions, and biological activity was evaluated using Pa (probability of being active) and Pi (probability of being inactive) values between 0.5 and 0.7.

2.3.2 Ligand and protein preparation

In this study, seven bioactive compounds of turmeric (cyclobisdmethoxy curcumin, Gibberellin A4, P,P Hydroxy curcumin**,** Curcumin, Pinocembrin, Piceatannol, and Demethoxyangonin) were tested against a protein known as the spike protein of SARS-CoV-2. The control medication used in this study was hydroxychloroquine, which is a reference drug in research on SARS-CoV-2, effective in entry inhibition. Although inactive clinically, it has proven in vitro activity on viral entry mechanisms, and so is a common positive control in most VLP and pseudovirus assays. The chosen ligands were created to reduce energy using PyRx's open Babel application after the 3D molecular structure of the ligands (hydroxychloroquine and bioactive chemicals) was recovered from PubChem chemical databases. The RCSB Protein Data Bank provided spike protein structures (7T67) with the target location sequence (D614G mutation). The RBD was chosen and saved as (.pdb). Discovery Studio 2016 client software was used to exclude water molecules and undesired ligands to produce these proteins.

2.3.3 Molecular docking and visualization

PyRx software version 0.8 was used for molecular docking. The Vina search box for the spike protein was configured for all docking procedures by targeting the active site, with dimensions in Angstroms set to x = 23.8194, y = 19.5605, and z = 25.0000. However, the center of the box was positioned at x = 125.8750, y = 195.8596, and z = 151.9893. Docking results were visualized using Discovery Studio software.

2.3.4 Molecular dynamics simulation

The YASARA (Yet Another Scientific Artificial Reality Application) program was used to conduct molecular dynamics simulations for 20 ns. The Amber14 force field was used, and the simulation parameters were set to approximate physiological circumstances (37°C, 1 atm, pH 7.4, and 0.9% salt content). The simulation was executed with the help of the MD run macro program, and the MD analysis and MD analysis macro programs were used to examine the outcomes.

2.4 In vitro study

2.4.1 Plasmid construction and cell culture

The protocol for plasmid construction was conducted based on previous research. The recombinant Spike (S), Membrane (M), and Envelope (E) proteins were expressed in human embryonic kidney 293T (HEK-293T) cells to produce the SARS-CoV-2 G614D virus-like particle (VLP). These proteins' sequences, which were gathered on April 14, 2020, were obtained from GISAID using the identifier hCoV-19/Indonesia/EJ-ITD3590NT/2020 (EPI_ISL_437188). A five-amino acid linker (PPVAT) was used to bind an enhanced green fluorescent protein (EGFP) to the carboxy terminus of the spike (S) protein to create a biological marker.

The EGFP protein sequence was retrieved from the NCBI GenBank database (accession number: U55761). These sequences were then optimized for human codon usage using the GenSmart Codon Optimization tool (GenScript) and synthesized into pcDNA3.1 (+) expression plasmids by GenScript (Singapore), resulting in three recombinant plasmids: Spike-EGFP_pcDNA3.1/Zeo(+), M_pcDNA3.1/Hygro(+), and E_pcDNA3.1/Zeo(+), which include zeocin and hygromycin antibiotic resistance genes to aid in the identification of successfully transfected cells. The HEK-293T cell line was obtained from Elabscience Biotechnology Inc. (USA). The cells were grown in Dulbecco's modified Eagle's medium (DMEM) with high glucose (Gibco; Thermo Fisher Scientific Inc., USA) supplemented with 10% fetal bovine serum (FBS) (Gibco; Thermo Fisher Scientific Inc., USA) and 1% of penicillin (100 U/mL) and streptomycin (100 μg/mL), and maintained at 37°C with 5% CO_2.

2.4.2 Transfection and isolation

Electroporation was used for transfection once HEK-293T cells surpassed 90% confluency. The cells were collected by trypsinization, centrifuged at 1,500 rpm for 5 min at 4°C, and rinsed with 500 μL of chilled phosphate-buffered saline (PBS). After homogenization, the cells were subjected to another round of centrifugation. Three recombinant plasmids (10 μL each) were introduced into the cells, homogenized, and placed in a cold electroporation tube. The mixture was kept cold for 5 min before being subjected to five pulses of electroporation at 1800 V, followed by a 10-min pause. Subsequently, the sample was transferred to a Petri dish and provided with a medium. Two days after transfection, the culture supernatant containing VLPs was collected into a 2 mL tube and subjected to stepwise centrifugation. The first spin was performed at 1,000 rpm for 10 min at 4°C. Then, a second spin was performed at 2,000 rpm for 10 min at 4°C. The liquid at the top was then filtered. The VLPs were separated from the filtered liquid using a 20% sucrose cushion at 39,000 rpm for 4 h at 4°C. The VLP-containing pellets were reconstituted in PBS. A NanoDrop spectrophotometer was used to measure VLP concentration.

2.4.3 Cytotoxicity assay

Vero E6 cell line was seeded into a 96-well plate at a concentration of 10,000 cells per well and incubated for 48 h. Then, the cells were exposed to different concentrations of *C. longa* ethanol extract (2.5, 5, 10, 20, and 40 μg/mL) separately. The cells were incubated at 37°C in a 5% CO_2 environment for 24 h. Following this, the treatment medium was replaced with one containing 5% Cell Proliferation Reagent WST-1 reagent (Roche Diagnostics GmbH, Germany) and incubated in the dark for 30 min. The absorbance was recorded using an ELx808 Absorbance Microplate Reader (BioTek Instruments) at 450 nm.

2.4.4 Analysis of VLP Internalization Inhibition

Preliminary inhibition testing of the extract was conducted to determine its ability to inhibit viral attachment to the host cell (Vero E6 Cell line). Vero E6- cells were seeded at a density of 6×10^4 cells per well in 24-well plates containing glass coverslips. The cells were cultured in DMEM with high glucose (Gibco; Thermo Fisher Scientific Inc., USA) supplemented with 10% fetal bovine serum (FBS) (Gibco; Thermo Fisher Scientific Inc., USA) and 1% penicillin (100 U/mL) and streptomycin (100 μg/mL). After 48 h (cell confluence > 60%), cells were treated with a mixture of turmeric and SARS-CoV-2 G614D VLP. The extract was prepared as a serial stock solution in DMSO and diluted five times in culture medium to a final concentration range from 2.5 μg/mL to 20 μg/mL (final DMSO concentration < 1%). SARS-CoV-2 VLPs were added at a final concentration of 100 μg/ml. The mixture was incubated for 30 min, added to the cells, and incubated for 30 min under the same conditions. The existing mixtures were removed, and the cells were washed three times with PBS. The culture was then observed under a fluorescence microscope (Olympus Fluoview FV1000). Treatments were performed in triplicate, and each culture was analyzed in four different fields of view. To quantify the inhibition of SARS-CoV-2 VLP attachment to the cells, the reduction in the intensity of the EGFP fluorescence area in the VLP-exposed cells was compared to the average intensity of the EGFP C+ control (VLP SARS-CoV-2, without extract) and C- control (without VLP SARS-CoV-2, without extract). ImageJ was then used to analyze the results.

2.4.5 Data Analysis

In vitro data are expressed as the mean ± standard deviation (SD) from three independent experimental replicates and then analyzed using One-way analysis of Variance (ANOVA) in IBM SPSS Statistics 20 software, USA.

3 Results and Discussion

3.1 In Silico studies

3.1.1 Bioactive Compounds Contained in C. longa

The compounds that satisfied the requirements for molecular docking and molecular dynamics simulation were identified using the LC-HRMS analysis. Through the use of

each compound's ionization method to increase or decrease the hydrogen atom, the mass error of each compound was counted and studied. According to the analysis, 24 turmeric components satisfied the requirements between 10 and 10 ppm (Table 1).

Table 1. Compounds list of *C. longa* from LC-HRMS analysis showing qualified mass error value

No	Compound	Formula	RT (min)	Theoretical m/z	Observed m/z	Mass Error (ppm)	CID	SMILES
1	2,3-Dihydro-1-benzofuran-2-carboxylic acid	C9 H8 O3	5.394	164.04668	164.04706	2.316414	2776555	C1C(OC2=CC=CC=C21)C(=O)O
2	16-Hydroxyhexadecanoic acid	C16 H32 O3	12.227	272.23512	272.23584	2.644773	10466	C(CCCCCCCC(=O)O)CCCCCCCO
3	Stearamide	C18 H37 N O	15.839	283.28695	283.28622	-2.576892	31292	CCCCCCCCCCCCCCCCCC(=O)N
4	NP-015687	C19 H16 O4	13.496	308.10417	308.10529	3.635134	118319242	C1C(OC(=CC1=O)/C=C/C2=CC=C(C=C2)O)C3=CC=C(C=C3)O
5	Curcumin	C21 H20 O6	11.139	368.1252	368.12626	2.879455	969516	COC1=C(C=CC(=C1)/C=C/C(=O)CC(=O)/C=C/C2=CC(=C(C=C2)O)OC)O
6	N,N-Diethyldodecanamide	C16 H33 N O	14.68	255.25585	255.25528	-2.233054	18783	CCCCCCCCCCCC(=O)N(CC)CC
7	Oleoyl ethanolamide	C20 H39 N O2	14.221	325.29753	325.29681	-2.213358	5283454	CCCCCCCC/C=C\CCCCCCCC(=O)NCCO
8	Ferulic acid	C10 H10 O4	5.828	194.05746	194.05697	-2.525025	445858	COC1=C(C=CC(=C1)/C=C/C(=O)O)O
9	6-Hydroxy-2-naphthoic acid	C11 H8 O3	9.998	188.04649	188.04722	3.882019	85557	C1=CC2=C(C=CC(=C2)O)C=C1C(=O)O
10	4-Hydroxybenzaldehyde	C7 H6 O2	4.488	122.03677	122.03601	-6.227631	126	C1=CC(=CC=C1C=O)O
11	Pinocembrin	C15 H12 O4	10.465	256.07338	256.07266	-2.811694	68071	C1[C@H](OC2=CC(=CC(=C2C1=O)O)O)C3=CC=CC=C3
12	(1E,4Z,6E)-5-hydroxy-1,7-bis(4-hydroxyphenyl)hepta-1,4,6-trien-3-one	C19 H16 O4	8.873	308.10436	308.10357	-2.564066	5324473	C1=CC(=CC=C1/C=C/C(=C/C(=O)/C=C/C2=CC=C(C=C2)O)/O)O
13	4-methoxy-6-[(E)-2-phenylethenyl]-2H-pyran-2-one	C14 H12 O3	10.424	228.07836	228.07763	-3.200654	5273621	COC1=CC(=O)OC(=C1)/C=C/C2=CC=CC=C2
14	Erucamide	C22 H43 N O	17.293	337.33357	337.33297	-1.778655	5365371	CCCCCCCC/C=C\CCCCCCCCCCCC(=O)N
15	Vanillin	C8 H8 O3	5.231	152.04718	152.04646	-4.735372	1183	COC1=C(C=CC(=C1)C=O)O
16	(-)-Caryophyllene oxide	C15 H24 O	11.007	220.18216	220.18144	-3.27002	1742210	C[C@@]12CC[C@@H]3[C@H](CC3(C)C)C(=C)CC[C@H]1O2
17	4'-Methoxyacetophenone	C9 H10 O2	7.596	150.06786	150.06713	-4.864466	7476	CC(=O)C1=CC=C(C=C1)OC
18	Veratrole	C8 H10 O2	6.992	138.06781	138.06709	-5.214829	7043	COC1=CC=CC=C1OC
19	Piceatannol	C14 H12 O4	7.522	244.07305	244.07238	-2.74508	667639	C1=CC(=C(C=C1/C=C/C2=CC(=CC(=C2)O)O)O)O
20	4-Methoxycinnamaldehyde	C10 H10 O2	6.678	162.06759	162.0672	-2.406403	641294	COC1=CC=C(C=C1)/C=C/C=O
21	Ethyl palmitoleate	C18 H34 O2	15.682	282.25559	282.25485	-2.621737	6436624	CCCCCC/C=C\CCCCCCCC(=O)OCC

22	2,4-Dimethylbenzaldehyde	C9 H10 O	14.157	134.07291	134.07223	-5.071867	61814	CC1=CC(=C(C=C1)C=O)C
23	Carvone	C10 H14 O	6.058	150.10422	150.1035	-4.796667	7439	CC1=CCC(CC1=O)C(=C)C
24	Gibberellin A4	C19 H24 O5	6.832	332.16243	332.16269	0.78275	92109	C[C@@]12[C@H](CC[C@@]3([C@@H]1[C@@H]([C@]45[C@H]3CC[C@H](C4)C(=C)C5)C(=O)O)OC2=O)O

3.1.2 Drug Likeness and Probable Activity Screening

Compounds with drug-like properties were chosen using drug likeness screening. Only seven of the 24 bioactive compounds from C. longa—curcumin, Pinocembrin, Piceatannol, P,P Hydroxy Curcumin, Cyclobisdmethoxycurcumin, Demethoxyyangonin, and Gibberellin A4—met the criteria for being considered medicinal substances (Figure 1(a)). The seven compounds from turmeric were continued to screen for probable bioactivity to predict the possibility of their activity in inhibiting SARS-CoV-2 (Figure 1(b)). The fact that compounds like curcumin, pinocembrin, piceatannol, and gibberellin A4 are identified is consistent with the reports that indicate their extensive biological properties, i.e., antiviral, antioxidant, and anti-inflammatory. Further predictions of PASS bioactivity further narrowed these candidates by assessment of their likelihood to have SARS-CoV-2-related inhibitory activity, with Pa between 0.5 and 0.7 representing noticeable chances of biological interest [8].

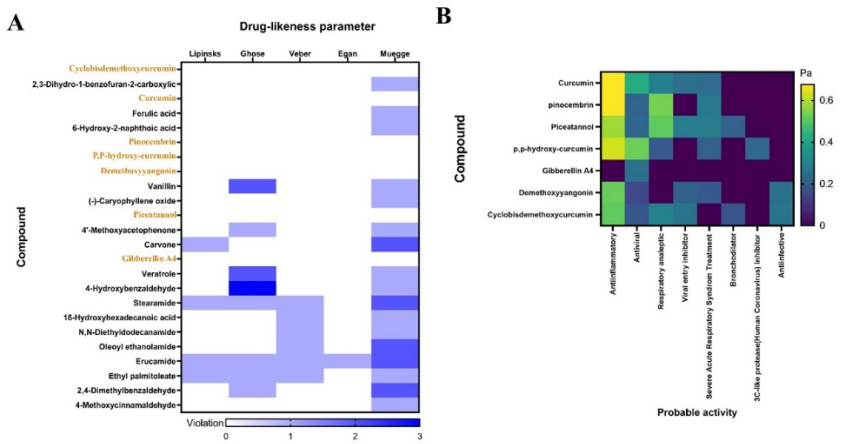

Fig. 1. The screening of drug likeness (a) and bioactivity screening (b) of turmeric (*C. longa*)

3.1.3 Molecular docking results

SARS-CoV-2's spike protein is one of several structural proteins that influence viral replication, which is essential to the virus's life cycle and could be a target for therapy. Preventing the spike protein from attaching to its ACE2 receptor and starting the virus's life cycle within the host is therefore crucial. After performing molecular docking, the interactions between ligands and protein were observed. Hydroxychloroquine was used as a pharmacological control for spiking protein [9], and the interaction between the

bioactive compounds of turmeric, as well as protein, was examined and classified based on binding affinity.

Table 2 shows that the binding affinity score of all *C. longa* bioactive substances was lower than that of hydroxychloroquine (control). Turmeric's ability to inhibit the SARS-CoV-2 protein is confirmed by the fact that cyclobisdmethoxy curcumin has the lowest binding affinity towards the spike protein (-7.035 kcal/mol). The binding affinity scores of P, P-Hydroxy Curcumin, Curcumin, Pinocembrin, piceatannol, and Desmethoxyyangonin against spike protein are lower than those of the control group (-5.461 kcal/mol) (-6.339, -6.258, -6.118, -5.81, and -5.52 kcal/mol, respectively). The intermolecular strength between the ligand and the protein decreases with decreasing binding affinity score, and the complex interactions that result are more stable [10]. These findings are in line with previous molecular docking studies that identify phytochemicals, particularly diarylheptanoids and polyphenols, as potent spike-RBD binders. These findings imply that turmeric may have antiviral effects through multi-target interactions rather than a single dominant molecule. However, docking only offers predictive data, and as in silico affinities do not necessarily correspond to biological activity, the higher binding scores should be regarded with caution. Therefore, to verify if these interactions take place under physiological settings, experimental validation utilizing pure chemicals is crucial [11].

Table 2. Turmeric bioactive compounds and the drugs control binding affinity towards the spike protein

Ligand	Binding affinity (kcal/mol)
Cyclobisdmethoxy Curcumin (118319242)	-7.035
P,P-Hydroxy-Curucumin (5324473)	-6.339
Curcumin (969516)	-6.258
Pinocembrin (68071)	-6.118
Piceatannol (667639)	-5.81
Desmethoxyyangonin (5273621)	-5.52
Hydroxychloroquine (3652) (control)	-5.461

3.1.4 Binding Interaction

The interaction of turmeric bioactive compounds with the spike protein is shown in Figure 2. Cyclobisdmethoxy Curcumin, P,P-Hydroxy Curcumin, Curcumin, Pinocembrin, Piceatannol, and Desmethoxyyangonin have lower binding affinity scores with spike protein than the control (Hydroxychloroquine). In addition to eleven van der Waals bonds formed by ILE472, PRO479, LYS458, GLN471, TYR473, PHE456, CYS480, LEU492, ARG454, SER469, and THR470, as well as one electrostatic bond with the amino acid residue ARG457 in the interaction of Cyclobisdmethoxy Curcumin with spike protein. P,P-Hydroxy phenyl curcumin and spike protein interaction resulted in the bond of two hydrogen bonds, which involved ASB481 and GLN474 amino acid residues as conventional hydrogen bonds, besides one electrostatic bond with ARG457 amino acid residue. Also formed one hydrophobic bond with PRO491 and eight van der Waals bonds formed by LYS458, GLU471, ILE472, TYR473, PHE456, SER469, THR470, and LEU492.

In addition, the interaction of Curcumin with spike protein formed four hydrogen bonds as conventional hydrogen bonds with GLN474, ARG457, GLU465, SER469, and one hydrogen bond as carbon hydrogen bond with SER459 amino acid residue, also formed one electrostatic bond with ARG457 and one hydrophobic bond with PRO491 as pi-alkyl, beside seven van der Waals bonds with LYS458, GLU471, THR470, ARG454, TYR473, ILE472, and PHE456 amino acid residue. While for Pinocembrin, with spike protein formed only two electrostatic bonds with GLU465, ARG457, and six van der Waals bonds with SER459, LYS458, PHE456, PRO491, TYR473, and GLU471. Moreover, Piceatannol interacts with the spike protein with two hydrogen bonds with SER469 and GLU471, and conventional hydrogen bonds, one hydrophobic bond with PRO491 as pi alkyl, one electrostatic bond with ARG457 as pi action, also nine van der Waals bonds with LYS458, GLU471, GLN474, TYR473, ARG454, THR470, LEU492, ASP467, ILE472, and PHE456. Lastly, methoxy-6-phenyl formed two hydrogen bonds and two hydrophobic bonds with LYS458 and TYR473. Besides six van der Waals bonds with GLN474, ILE472, ARG457, PHE456, PRO491, and GLU471 amino acid residues, with an interaction with the spike protein.

In complex ligand-protein interactions, the fundamental role of hydrogen bonding is crucial. In order to optimize the complex required to enhance the ligand's molecular weight, lipophilicity, and ADMET characteristics, the high number of hydrophobic interactions was investigated. Turmeric is a more suited complex ligand-protein than the complex between antiviral medications and protein, as evidenced by the large number of hydrogen bonds and hydrophobic contacts of the bioactive chemicals against the protein. These patterns of interaction suggest that phytochemicals derived in turmeric establish a variety of stable interactions with essential residues in the spike-RBD, which is consistent with previous molecular docking data that natural polyphenols and diarylheptanoids could effectively stabilize spike-ligand complexes by forming hydrogen bonds and hydrophobic interactions. These multi-point interactions provide the idea that turmeric can have antiviral effects by the multiple-target interaction but not by one mechanism. Molecular docking, however, can only offer predictive evidence, and the scores of bindings are not always correlated with the activity of a substance. Thus, the use of isolated compounds is also crucial to check whether these predicted interactions can take place under physiological conditions [12]. As a result, turmeric as an anti-viral medicine against SARS-CoV-2 is more successful than anti-viral drugs.

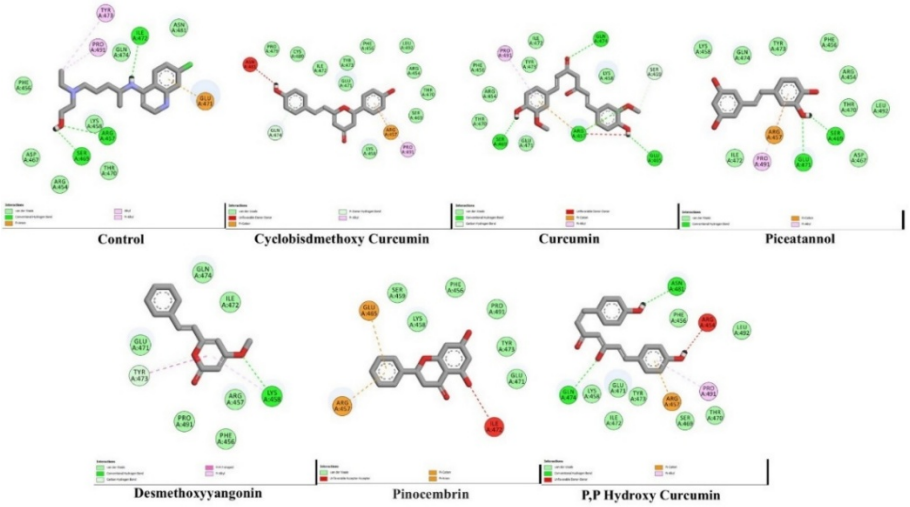

Fig. 2. Binding Interaction of turmeric bioactive compounds with spike protein

3.1.5 Molecular dynamics simulation of turmeric

Molecular dynamics simulation was used to analyze the stability of the interaction between the Spike protein and compounds**.** Based on Figure 3, turmeric bioactive compounds like curcumin and Pinocembrin) show the least fluctuation and the lowest RMSD values, indicating the most stable binding with the spike proteins, compared with the control, which shows the highest instability, especially after 10 ns. Besides that, Hydroxy curcumin and Methoxy-6-phenyle exhibit better stability than the control. So, turmeric bioactive compounds can inhibit the spike protein. It is also indicative in these MD results that the stability of turmeric-derived ligand-protein complexes is more than that of hydroxychloroquine and, indeed, in line with other computational studies which have reported that curcumin analogs stabilize SARS-CoV-2 spike complexes by stabilizing their hydrogen bonds and their conformational dynamics [13]. The low RMSDs herein suggest that the compounds have constant binding poses in the course of the simulation which would qualify them as effective spike inhibitors. Nonetheless, since MD is predictive evidence, it needs to be validated through experimentation whether these stable interactions occur under physiological states.

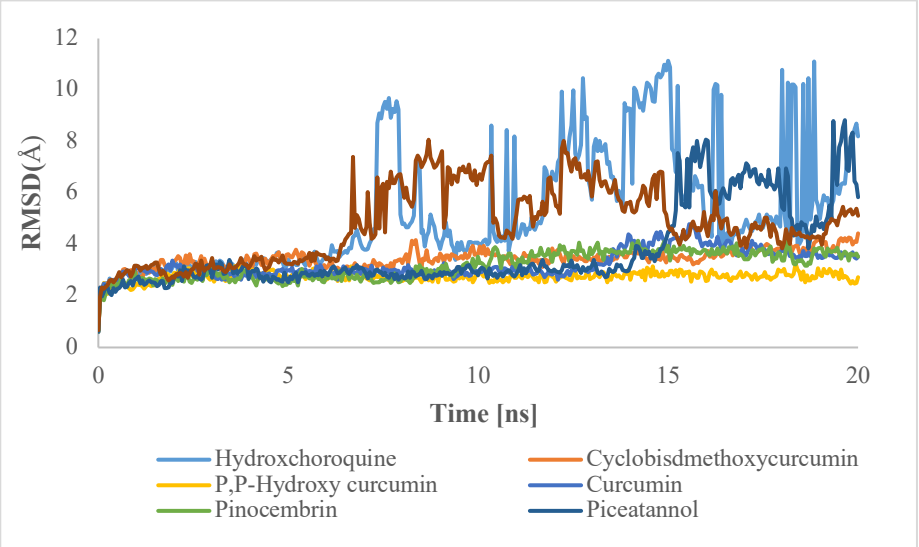

Fig. 3. RMSD of turmeric bioactive compounds and control against spike protein

The flexibility of protein residues upon ligand binding was evaluated using Root Mean Square Fluctuation (RMSF) analysis. Among them, hydroxycurcumin and curcumin demonstrated the lowest RMSF values, particularly at THR470 and GLU471, indicating more stable binding interactions than the control drug (Figure 4). These results support the potential of green tea and turmeric compounds to maintain stable binding with the spike protein and inhibit viral activity.

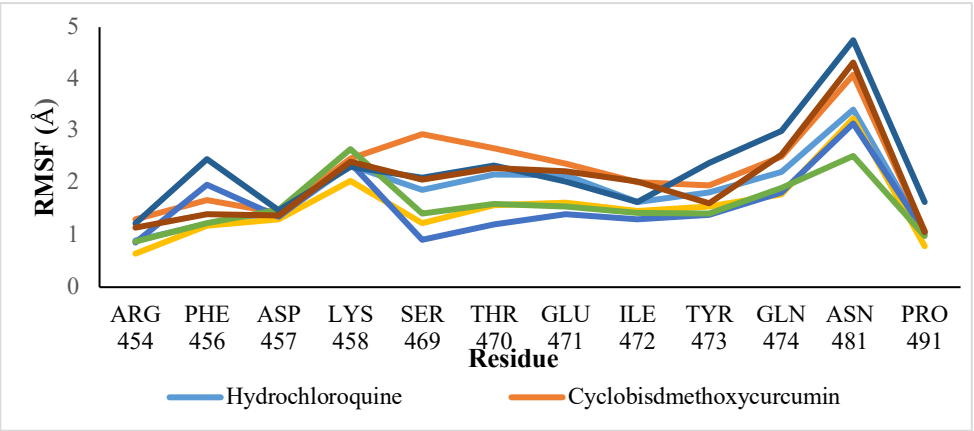

Fig. 4. RMSF of the turmeric bioactive compounds and control against the spike protein

3.2 In vitro studies

3.2.1 Cytotoxicity of Turmeric (C. longa) Extract on Vero E6 Cells

Figure 5 shows that *C. longa* extract showed a more pronounced concentration-dependent reduction in cell viability. At 2.5 µg/mL, viability was 85.9% and decreased further at 5 µg/mL (78.0%). At 10 µg/mL, cell viability slightly improved to 83.5% but

declined again at 20 μg/mL and 40 μg/mL, reaching 76.4% and 75.3%, respectively. Although viability remained above 70% at all tested doses, the results indicate that *C. longa* extract exerts a moderate cytotoxic effect. This finding is consistent with previous research showing that curcumin, the main active compound in turmeric, can reduce Vero E6 cell viability in a dose-dependent manner when tested using MTT assays, while still maintaining >80% viability at lower concentrations relevant for antiviral testing [14]. These trends indicate that although turmeric extract can be considered overall safe at low doses, higher doses of the extract can cause cellular stress reactions or instability of the compounds, which can affect antiviral effects. Consequently, it is important to choose an ideal non-toxic range of concentration that excludes such factors as cytotoxicity, which may confound antiviral effects. Turmeric (*C. longa*) extract can be used within a non-toxic concentration range but may require more careful dose selection.

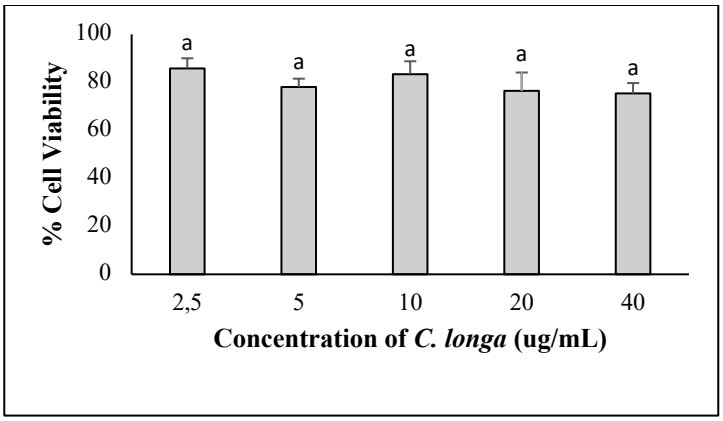

Fig. 5. Cytotoxicity of Turmeric Extract on Vero E6 Cells

3.2.2 The Inhibitory Effect of Turmeric (C. longa) on VLP Attachment in Vero E6 Cells

The fluorescence microscopy images showed strong EGFP fluorescence in the positive control (K+, VLP SARS-CoV-2 without extract), while the negative control (K–) exhibited minimal background fluorescence. Treatment with turmeric extract for 24 h produced a distinct dose–response pattern. At 2.5 and 5 μg/mL, EGFP intensity was strongly reduced compared to the positive control, indicating inhibition of VLP attachment. However, increasing the concentration to 10 and 20 μg/mL resulted in higher EGFP intensity compared to the lower doses, approaching the positive control levels. This suggests that at higher concentrations, turmeric extract may allow increased VLP entry, possibly due to cytotoxic effects altering cell membrane integrity or other cellular processes. Phase-contrast images supported this observation, as some morphological stress was observed at 10 and 20 μg/mL. These results indicate that turmeric extract exerts its strongest inhibitory effect at lower concentrations, while higher doses may reduce its antiviral activity (Figure 6 (a) and (b)).

These results are in line with previous investigations demonstrating the broad-spectrum antiviral action of curcumin, the main bioactive component of turmeric,

including against SARS-CoV-2. By attaching to the primary protease (Mpro) and disrupting spike–ACE2 receptor connections, curcumin has been shown to prevent viral propagation (Manoharan et al., 2020). Molecular docking and in vitro assays have further demonstrated curcumin's ability to disrupt essential viral proteins, thereby preventing viral entry and replication. However, several studies have also highlighted that curcumin suffers from poor solubility and bioavailability at higher concentrations, which may explain the diminished efficacy we observed at 10 and 20 µg/mL [15]. These results suggest that turmeric (*C. longa*) extract was most effective in suppressing SARS-CoV-2 VLP entry at low concentrations, while higher doses may compromise antiviral effects due to cytotoxicity and compound instability. Nevertheless, these results must be viewed with some hesitation, since the crude extract and VLP entry model used are significant limitations that do not entirely reflect the active compounds involved, and the entire viral replication cycle in question.

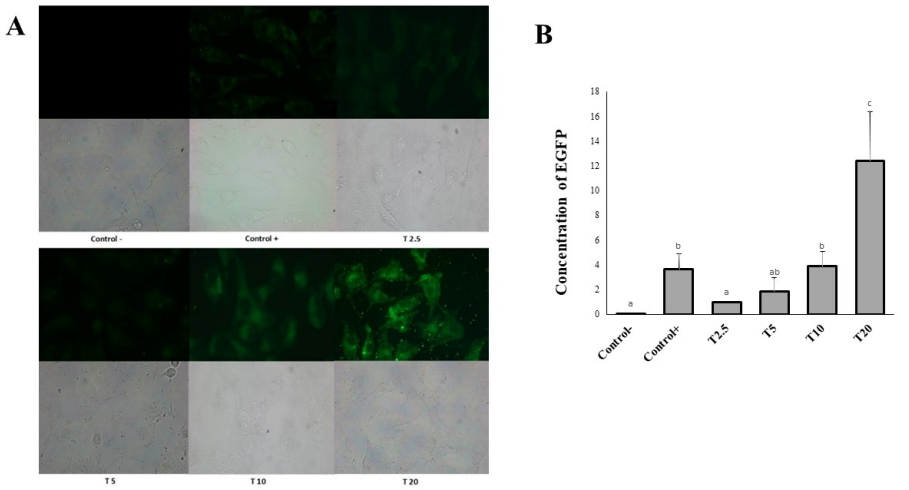

Fig. 6. In vitro evaluation of turmeric extract's ability to prevent SARS-CoV-2 VLPs from adhering to Vero E6 cells. A. The observation of EGFP fluorescence on SARS-CoV-2 VLP-exposed Vero E6 cells using fluorescent microscopy. B. The fluorescent intensity of EGFP in SARS-CoV-2 VLP-exposed Vero E6 cells after being treated with turmeric at 2.5 (T2.5), 5 (T5), 10 (T10), and 20 (T20) µg/mL.

4 Conclusion

The current work emphasizes turmeric's (C. longa) potential as a natural antiviral strategy against SARS-CoV-2 D614G VLPs. When compared to the control drug, the in silico investigation showed that several types of compounds derived from turmeric, especially curcumin and its analogs, showed favorable binding affinity and stable interactions with the spike protein. These findings were further supported by molecular dynamics simulations, which confirmed the stability of the ligand–protein complexes. In vitro experiments using Vero E6 cells revealed that turmeric extract significantly inhibited viral entry at lower concentrations (2.5–5 µg/mL), while higher concentrations reduced

antiviral activity, likely due to moderate cytotoxic effects. These results indicate that turmeric bioactive compounds possess dual potential as antiviral agents by interfering with spike protein function and preventing viral attachment. Nevertheless, further investigations, including in vitro and in vivo validation and formulation strategies to improve bioavailability, are required to establish turmeric as a complementary therapeutic option against SARS-CoV-2 infection.

Acknowledgements
The authors express their gratitude to Universitas Brawijaya for providing financial support for this research under the Professor Research Grant (grant no. 06871.4/UN10.F0901/B/PT/2025) and supporting the Doctoral Program of the first author.

Fundings
This research was funded by Universitas Brawijaya under the Professor Research Grant (grant no. 06871.4/UN10.F0901/B/PT/2025).

Data availability statement
The data that support the findings of this study are available from the corresponding author upon reasonable request.

Author contribution statement
Hagar Ali Marzouk: Conceptualization, Methodology, Investigation, Writing- Original draft preparation. Marlita Marlita: Data curation, Writing- Original draft preparation. Kavana Hafil Kusuma: Investigation, Writing- Original draft preparation. Yuyun Ika Christina: Validation, Writing- Reviewing and Editing. Aries Soewondo: Validation, Writing- Reviewing and Editing. Sri Rahayu: Validation, Writing- Reviewing and Editing. Nashi Widodo: Conceptualization, Methodology, Supervision, Validation, Writing- Reviewing and Editing. Muhammad Sasmito Djati: Conceptualization, Methodology, Supervision, Validation, Writing- Reviewing and Editing.

References

1. S. Ahmad, S. Zahiruddin, B. Parveen, P. Basist, A. Parveen, Gaurav, R. Parveen, and M. Ahmad, Front Pharmacol 11, (2021)
2. W. Ma, K. Zhang, Y. Cao, and M. Li, Natl Sci Rev 12, (2025)
3. F. S. Alhamlan and A. A. Al-Qahtani, Int J Mol Sci 26, 1263 (2025)
4. A. J. Zak, T. Hoang, C. M. Yee, S. M. Rizvi, P. Prabhu, and F. Wen, Int J Mol Sci 24, 14622 (2023)
5. I. Petrovskis, D. Skrastina, J. Jansons, A. Dislers, J. Bogans, K. Spunde, A. Neprjakhina, J. Zakova, A. Zajakina, and I. Sominskaya, Vaccines (Basel) 12, 267 (2024)
6. D. Marín-Palma, J. H. Tabares-Guevara, M. I. Zapata-Cardona, L. Flórez-Álvarez, L. M. Yepes, M. T. Rugeles, W. Zapata-Builes, J. C. Hernandez, and N. A. Taborda, Molecules 26, 6900 (2021)
7. H. Alici, Pharmaceuticals 18, 798 (2025)
8. K. Rajagopal, P. Varakumar, A. Baliwada, and G. Byran, Futur J Pharm Sci 6, 104 (2020)
9. S. Sandeep and K. McGregor, (2020)
10. A. Ahmed, B. Mam, and R. Sowdhamini, Bioinform Biol Insights 15, (2021)
11. A. Nag, R. Banerjee, S. Paul, and R. Kundu, Comput Biol Med 146, 105552 (2022)

12. I. Luque Ruiz and M. Á. Gómez-Nieto, J Chem Inf Model 58, 2069 (2018)
13. S. Rampogu, G. Lee, J. S. Park, K. W. Lee, and M. O. Kim, Int J Mol Sci 23, 1771 (2022)
14. Y. Manoharan, V. Haridas, K. C. Vasanthakumar, S. Muthu, F. F. Thavoorullah, and P. Shetty, Indian Journal of Clinical Biochemistry 35, 373 (2020)
15. B. Salehi, D. Calina, A. Docea, N. Koirala, S. Aryal, D. Lombardo, L. Pasqua, Y. Taheri, C. Marina Salgado Castillo, M. Martorell, N. Martins, M. Iriti, H. Suleria, and J. Sharifi-Rad, J Clin Med 9, 430 (2020)